Surface-initiated Atom Transfer Radical Polymerization and Solution Intercalation Methods for Preparation of Cellulose-G-PS-G-PAN/MMT Bionanocomposite

Mousa Pakzad [1], Ali Ramezani [1], and Mojtaba Abbasian*[2]

[1] Faculty of Science, University of Zanjan, Zanjan, Iran
[2] Department of Chemistry, Payame Noor University (P.N.U), P.O.Box,19395-3697 Tehran, Iran

ABSTRACT

Cellulose was modified by polystyrene (PS) and polyacrylonitrile (PAN) via free radical and living radical polymerization, and then cellulose was used as the matrix in the preparation of polymer/clay nanocomposite, through a solution intercalation method. For this purpose, first, the graft polymerization of styrene (St) onto cellulose fibers was performed by using suspension polymerization and the free-radical polymerization technique in the presence of potassium persulfate (PPS). Second, the synthesized cellulose-graft-polystyrene was brominated by N-bromosuccinimide (NBS) to obtain polymers with bromine a group. Third, the brominated cellulose fibers were used as macroinitiators in the atom transfer radical polymerization (ATRP) of acrylonitrile (AN) in the presence of CuCl / 2, 2'-bipyridine (Bpy) catalyst system in THF solvent at 90˚C to prepare the cellulose-graft-polystyrene-graft-polyacrylonitrile. Forth, for preparing the modified clay, Na-MMT was mixed with hexadecyl trimethyl ammonium chloride salt. Finally, cellulose-graft-polystyrene–graft–polyacrylonitrile/organoclay bionanocomposite was prepared in CCl_4 by a solution intercalation method. Then, the structure of the obtained terpolymer was investigated by FT-IR, DSC, TGA, XRD, and SEM techniques. Moreover, the structure of the bionanocomposite was probed by XRD, SEM, and TEM images.

Key words: Bionanocomposite, Cellulose, Styrene, Atom Transfer Radical Polymerization, Modified Clay

INTRODUCTION

In recent years, special attention has been paid to the benefits of polymer nanocomposite technology to improve the inherent properties of biodegradable polymers [1-3]. These materials are called "bionanocomposites," and they provide a fascinating interdisciplinary research field which combines materials science with nanotechnology and biological sciences. The composites based on biodegradable polymers and different nanofillers with varying functionalities can lead to bionanocomposites with applications ranging from environmentally friendly packaging to automotive uses [4].

Bionanocomposites based on nanoclays or layered silicates and biodegradable polymers have attracted greater interest in today's materials

*Corresponding author

Mojtaba Abbasian

Email: m_abbasian@pnu.ac.ir

Tel:+98 41 35492301

Fax:+98 41 35492301

http://jpst.ripi.ir

research because it is possible to achieve impressive enhancements of the properties of the polymers when compared with virgin polymers [5-6]. These improvements can include high moduli, increased strength and heat resistance, decreased gas/vapor permeability and flammability, and increased degradability of biodegradable polymers [7].The most representative layered silicate is natural montmorillonite (MMT), which consists of regular stacks of aluminosilicate layers with a high aspect ratio and a high surface area. Cellulose is the most abundant natural polymer in nature, and it is currently one of the most promising polymeric resources, being the component of paper, textiles, membranes, artificial fibers, etc. Cellulose, which is a linear polymer of β-1, 4-linked D-glucopyranose monomers, has many attractive properties; such as, biodegradability, renewability, biocompatibility, non-toxicity, and low cost [10, 11]. However, the processing of cellulose is difficult in general. Cellulose is neither meltable nor soluble in water or common solvents due to its partially crystalline structure and close chain packing via numerous inter- and intra-molecular hydrogen bonds [12, 13]. To overcome such drawbacks, the chemical modification of the cellulose structure is necessary [14]. Graft copolymerization is a commonly used method for the modification of surfaces of polymers; in addition, it is an important tool in order to modify the physical or chemical properties of polymers. By grafting hydrophobic polymer chains onto the cellulose fiber surface, the hydrophilicity of the cellulose can be altered. Furthermore, by grafting functional polymers, a function can be introduced into cellulose, allowing for cellulose to be utilized in advanced material applications [15,16]. In general, graft copolymers can be synthesized by free radical-induced grafting processes, which are the easiest and the most widely accepted procedures [17]. However, one of the major limitations of this technique is the formation of unwanted homopolymer, which usually proceeds into parallel with the graft copolymerization. In addition, the free radical technique produces many radicals simultaneously, which leads to complex reactions, including chain transfer and chain termination reactions. Therefore, there is a lack of control over molecular weight and polydispersity of the graft chains [18]. These problems can be circumvented through applying of living radical polymerization methods; such as, nitroxide-mediated polymerizations (NMP) [19,21], reversible addition–fragmentation chain transfer polymerization (RAFT) [22-24], and atom transfer radical polymerizations (ATRP) [25-27]. Metal-catalyzed living-radical polymerization, generally called atom-transfer radical polymerization (ATRP), is one of the most widely used methods for controllable radical polymerization; moreover, metal-catalyzed living-radical polymerization is based on the reversible reaction of low oxidation-state metal complexes with an alkyl halide, generating radicals and the corresponding high-oxidation state metal complexes with a coordinated halide ligand [28]. The methods typically used to prepare biopolymer/layered silicate bionanocomposites involve the incorporation of a layered silicate into a solvent-swollen polymer (solution blending) [29], polymer melt (melt blending) [30], or the addition of a modified silicate to a polymerization reaction (in situ method) [31]. Because cellulose has numerous hydroxyl functional groups which result in strong hydrogen bonds, it tends to decompose at temperatures below its melting point; therefore, we have opted for the living free radical polymerization

and solution casting technique instead of melt compounding to prepare grafted cellulose/clay bionanocomposites. ATRP was used to synthesize graft copolymer on the backbone of cellulose with acrylonitrile monomers (AN). For this purpose, first, styrene (St) has been grafted onto cellulose fibers by using suspension polymerization and the free-radical polymerization technique. Potassium persulfate (PPS) has been used as a chemical initiator, and water was used as a medium. We used cellulose-graft-polystyrene (Cell-g-PS) as a starting polymer and N-bromosuccinimide (NBS) as a brominating agent to obtain polymer with bromine groups. This brominated cellulose fibers have been used as an ATRP macroinitiator. This macroinitiator can polymerize AN in the presence of CuCl / 2, 2'-bipyridine (Bpy) catalyst system in THF solvent at 90°C to prepare the cellulose–graft-polystyrene–graft–polyacrylonitrile (Cell-g-PS-g-PAN). Clay (Na-MMT) has been treated via hexadecyl trimethyl ammonium chloride salt to obtain modified clay (O-MMT). Finally, cellulose–graft–polystyrene–graft polyacrylonitrile/organoclay bionanocomposite has been prepared in CCl_4 by a solution intercalation method. The structure of the obtained terpolymer has been investigated by FT-IR, DSC, TGA, XRD, and SEM techniques. The structure of the nanocomposite has been probed by XRD, SEM, and TEM images.

EXPERIMENTALS PROCEDURES

Materials

St (Merck Co.) has been distilled under a reduced pressure before use. AN (Aldrich Co.) has been washed with 8% NaOH followed by distilled water and dried over anhydrous sodium sulfate. Hexadecyl trimethyl ammonium chloride salt (Merck Co.) was used as received. Sodium montmorillonite (MMT) has been obtained from Southern Clay Products, under the trade name of Cloisite NaC. MMT is reported to have an approximate aspect ratio of 250:1 and is a 2:1 tetrahedral/octahedral aluminum silicate smectite mineral with an idealized chemical formula of $Na_{0.33}[Mg_{0.33}Al_{11.67} Si_4O_{10}](OH)_2$ and a cation exchange capacity of 95 meq/100 g. Microcrystalline cellulose (MCC) from Merck Co. has been pretreated with 16% NaOH, and has then been used. AIBN has been recrystallized from ethanol, and then dried at room temperature in a vacuum oven; finally, AIBN has been stored in a freezer. Bpy (Merck Co.) has been used as received. Copper (I) chloride (Merck Co.) was purified by stirring in glacial acetic acid, then washed with methanol, and finally dried under reduced pressure. THF (Merck Co.) were dried by refluxing over sodium and distilled under argon before use. All other reagents were purchased from Merck Co.

Instrumentation

Fourier-transform infrared (FTIR) spectra of the samples were obtained on a Shimadzu 8400 S FTIR (Shimadzu, Kyoto, Japan). The samples were prepared by grinding the dry powders with KBr and compressing the mixture into disks. The disks were stored in a desiccator to avoid moisture absorption. The spectra were recorded at room temperature. Thermogravimetric analysis (TGA) of the nanocomposite was obtained with METTLER-TOLEDO 851e (METTLER-TOLEDO, USA) instrument. About 10 mg of the sample was heated between 25 and 600°C at a rate of 10°C min-1 under flowing nitrogen. Differential scanning calorimetry analyses were performed on a METTLER-TOLEDO 822e (METTLER-TOLEDO, USA) instrument. The sample was first heated to 200°C and then allowed to cool for 5 min to eliminate the thermal history. Thereafter, the

sample was reheated to 200°C at a rate of 10°C min⁻¹. The entire test was performed under nitrogen purging at a flow rate of 50 mL/min. X-ray diffraction (XRD) spectra were obtained by using a Siemens D 5000, X-ray generator (Siemens, USA) (CuKα radiation with λ=1.5406 A°) with a 2θ scan range of 2°C to 80°C at room temperature. The morphology of the samples was obtained by scanning electron microscopy (SEM) (Model S360 Mv2300, England) instrument. Transmission electron microscopy (TEM) was performed using a Philips CM[10] microscope (Phillips, Eindhoven, Netherlands) at an accelerating voltage of 100 kV.

St Growing onto Cellulose Backbone by Free Radical Polymerization

A mixture of cellulose [4 g, 2.47 mmol, based on the anhydroglucose (AHG) unit] and 40 mL distilled water was stirred in a two-neck flask under nitrogen atmosphere and at the reaction temperature for 30 min to obtain homogeneous slurry. After adding PPS for 10 min, St was added. Water was 100 mL, while the total amount of cellulose and St was 10 g. The graft copolymerization parameters included cellulose:St ratio (1:3 by weight), PPS content (0.2–1.2 g), reaction time (1–5 hr.), and reaction temperature (30-60°C). The nitrogen atmosphere and the agitation of slurry were maintained throughout the experiment. After the reaction time was over, the slurry was dropped into methanol. The precipitate was filtered, washed with methanol, dried in an oven at 50°C until a constant weight was achieved, and kept in desiccators. Soxhlet extraction with toluene was applied to the precipitate for removing St homopolymer. The extraction was done at 120°C for 10 hrs. Additionally, the extracted solution was dropped into methanol which is a non-solvent of PS. The cellulose-graft-polystyrene (Cell-g-PS) copolymer was dried in a vacuum oven at 60°C until a constant weight was obtained and was kept in the desiccators (For cellulose: FTIR (KBr) υ: 3334, 2890, 900-1163 cm⁻¹; for Cell-g-PS: FTIR (KBr) υ: 1448, 1491, 1530 and 1635 cm⁻¹).

Synthesis of ATRP Macroinitiator (Brominated Cell-G-PS)

Cell-g-PS (8 g, 30.18 mmol) was dissolved in CCl_4 (100 ml) and NBS (1 g, 5.62 mmol) and AIBN (0.06 g, 0.37 mmol) were added; then, the mixture was refluxed under stirring. The reaction solution became brownish under foaming. After 4 hrs heating, the succinimide was filtered off; the filtrate was concentrated in vacuo and poured into methanol. The brominated polymer precipitated as powder. This was separated by filtration and dissolved again in dichloromethane (DCM). This solution was centrifuged in order to remove some insoluble matter and poured again in methanol. This purification process was repeated three times. The purified brominated Cell-g-PS product was dried in the vacuum oven at 60°C for 2 days (FTIR (KBr) υ: 1446, 1489, 1595, and 804 cm⁻¹).

Polymerization of AN onto Cell-G-PS Copolymer by ATRP

In a two-necked flask equipped with a magnetic stirrer, a mixture of THF (30 mL) and CuCl (0.02 g, 0.2 mmol) was stirred under argon atmosphere for 10 min. Then, the AN (8 mL, 0.12 mmol) and Bpy (0.06 g, 0.38 mmol) were added into the mixture. After that, macroinitiator (brominated Cell-g-PS) was added into flask, and the mixture was degassed and sealed under vacuum for 15 min and maintained at 80-90°C for about 48 hrs. At the end of the reaction, the mixture was washed with methanol and filtered, and the product was dried.
in the vacuum oven at 60°C for 2 days. The dried product was extracted with DMF (100 mL) for 48 hrs

to remove the homopolymer (PAN). (FTIR (KBr) υ: 2243, 1645 cm^{-1}).

Synthesis of O-MMT

Organo-modified MMT (O-MMT) was obtained after that, MMT was treated with hexadecyl trimethyl ammonium chloride salt via an ion-exchange process. MMT was first dispersed in deionized water under ultrasound for 1 hr. Second, the modifier was prepared in deionized water separately, and third the modifier was added to the clay dispersion at an amount a little higher than the cation exchange capacity (CEC) of MMT. Forth, the resultant suspension was intensively stirred for 10 hrs. Fifth, the resultant suspension was filtered with deionized water three times. Ultimately, the final product was dried in vacuum at room temperature for 48 hrs after which it was grounded into powder prepared in deionized water separately, and third the modifier was added to the clay dispersion at an amount a little higher than the cation exchange capacity (CEC) of MMT. Forth, the resultant suspension was intensively stirred for 10 hrs. Fifth, the resultant suspension was filtered with deionized water three times. Ultimately, the final product was dried in vacuum at room temperature for 48 hrs after which it was grounded into powder.

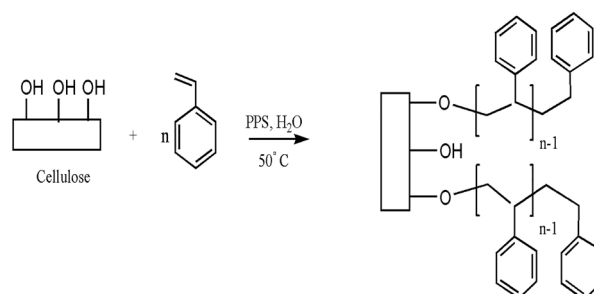## Synthesis of Bionanocomposite

First, 0.1 g of organoclay montmorillonite (3 wt.%) was dispersed in 30 mL of carbon tetrachloride for 30 min under ultrasound, after which 2 g of Cell-g-PCMSt-g-PAN was dissolved in 50 mL carbon tetrachloride; then, clay suspension was slowly added to polymeric solution at constant stirring for 6 hrs. Afterwards, the mixture was poured into 300 mL methanol for rapid precipitation. The precipitate was filtered and dried at 50°C under
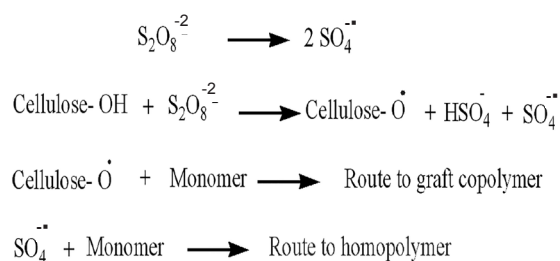
vacuum for 2 days.

RESULTS AND DISCUSSION

St Growing onto Cellulose Backbone by Free Radical Polymerization

Radical polymerization [32] is a chain reaction process consisting of mainly three steps; initiation, propagation, and termination. The chains are initiated by initiator derived radicals and add to monomers. The subsequent addition of monomers to the propagating radical is the basis of the step of chain propagation. A chain termination takes place when the propagating radicals react by combination, disproportionation, and transfer. In the free radical graft copolymerization of cellulose, free radicals on the cellulosic backbone can be formed by chemical initiators [33] or by (IR) radiation [34]. In the present work, Cell-g-PS has been synthesized via free-radical polymerization of St by using suspension polymerization technique (Scheme 1). PPS has been used as a chemical initiator, and water was used as a medium. Initiation via PPS involves the generation of the initiating species on the swollen cellulose substrate backbone. This is usually carried out by saturating the cellulose substrate with PPS [35]. The mechanism of PPS initiation is shown in Scheme 2 [36].

Scheme 1: Synthesis of (Cell-g-PS)

$$S_2O_8^{-2} \longrightarrow 2\,SO_4^{\cdot\cdot}$$

$$\text{Cellulose-OH} + S_2O_8^{-2} \longrightarrow \text{Cellulose-}\overset{\cdot}{O} + HSO_4^{\cdot} + SO_4^{\cdot\cdot}$$

$$\text{Cellulose-}\overset{\cdot}{O} + \text{Monomer} \longrightarrow \text{Route to graft copolymer}$$

$$SO_4^{\cdot\cdot} + \text{Monomer} \longrightarrow \text{Route to homopolymer}$$

Scheme 2: A simplified mechanism for the graft polymerization of cellulose in the presence of PPS as a free radical polymerization catalyst.

FT-IR spectra of the unmodified cellulose (a) and Cell-g-PS (b) are shown in Figure 1.
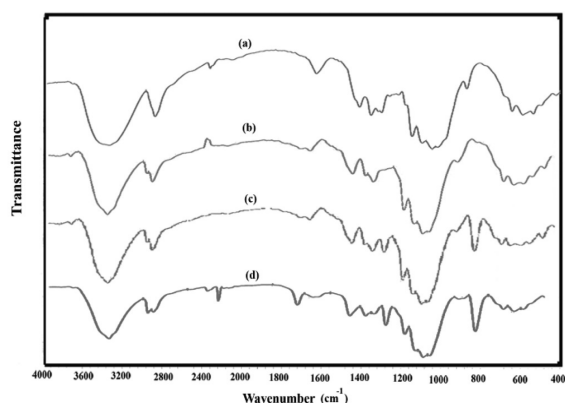
Figure 1: FT-IR spectra: (a) pure cellulose, (b) Cell-g-PS, (c) brominated (Cell-g-PS), and (d) Cell-g-PS-g-PAN.

The FT-IR spectrum of unmodified cellulose shows the characteristic absorption due to the stretching vibration of OH and −CH of CH_2OH group (3334, 2890 cm^{-1}) and C-O stretching vibration (900-1163 cm^{-1}). The FT-IR spectra of Cell-g-PS shows the characteristic absorption due to the stretching vibration of aromatic -CH (3032 cm^{-1}), phenyl ring stretching vibration (1448, 1491, 1530 cm^{-1}), and aromatic -C=C stretching vibrations (1635cm^{-1}).

## Synthesis of ATRP Macroinitiator (Brominated Cell-G-PS)

To get ATRP initiator, the Cell-g-PS was brominated with NBS using AIBN as the catalyst. It is obvious that the bromination occurs by this process radically at the α-carbon to the benzene nucleus. Figure 1(c). shows the FT-IR spectrum of the brominated Cell-g-PS. The FT-IR spectrum shows the characteristic absorption due to the stretching vibration of aliphatic and aromatic -CH (3010, 2890 cm^{-1}) and phenyl ring stretching vibration (1446, 1489, 1595 cm^{-1}), and the peak at 804 cm^{-1} is attributed to the CH_2Br of St.

Polymerization of AN onto Cell-G-PS by ATRP

In the present study, ATRP technique was employed for the first time to prepare graft copolymer by having Cell-g-PS as a backbone and PAN as branches Brominated Cell-g-PS can polymerize AN in the presence of CuCl/Bpy catalyst system in THF at 90°C to prepare Cell-g-PS-g-PAN (Scheme 3).

Figure 1(d) shows the FT-IR spectrum of Cell-g-PS-g-PAN. The characteristic absorption due to the stretching vibration of −CN group (2243 cm^{-1}), the stretching vibration of OH group (3344 cm^{-1}), the stretching vibration of aliphatic and aromatic −CH(3018, 2902 cm^{-1}), and the peaks at 802 and 1645 cm^{-1} were attributed to CHBr and aromatic -C=C.
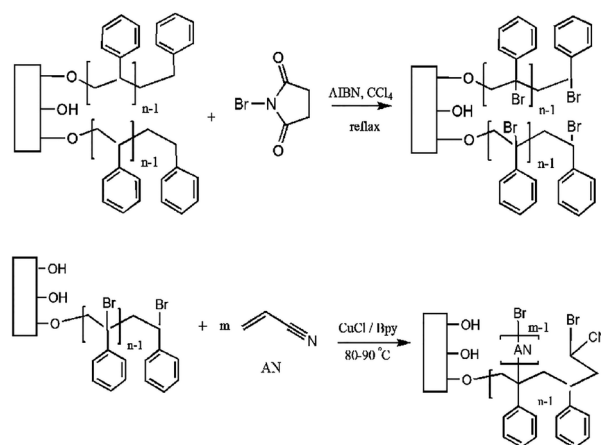
Scheme 3: Preparation of Cell-g-PS-g-PAN

XRD Analyses

The X-ray diffraction patterns of Cell-g-PS-g-PAN terpolymer were detected as illustrated in Figure 2.
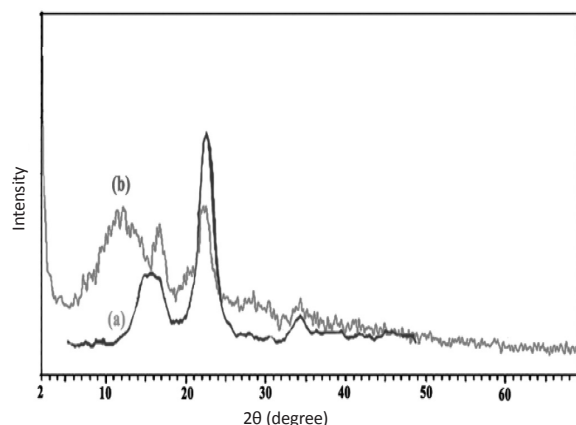
**Figure 2: XRD patterns of (a) pure cellulose and
 (b) Cell-g-PS-g-PAN**

It was known that the diffraction pattern of original cellulose shows the characteristic peaks at $2\theta = 22°$ [37], whereas for grafted terpolymer, this peak has almost been decreased, which indicates a remarkable decrease in crystallinity in the graft terpolymer. This may be attributed to the introduction of bulky chains of grafted PS in cellulose matrix. The good conjugation of PS with cellulose markedly disordered the pure cellulose at a molecular level, leading to the low crystallization of the terpolymer.

Thermal Analysis

TGA thermograms and DSC curves of the unmodified cellulose and Cell-g-PS-g-PAN are shown in Figures 3 and 4 respectively. In Figure 3, we can point out the following characteristic behaviors. In low temperature regions showed in Figure 3, at $250°C$, the mass loss was 10% for cellulose [37], while it was lower than 5% for terpolymer. Endothermic peaks are observed for cellulose [38] and terpolymer samples at around $98°C$, which became smaller with the increase of grafting. Thus the aforementioned mass losses at this stage can be attributed to the desorption of water. In the temperature range of $250–370°C$, there is also a certain difference between TGA thermograms and DSC curves for cellulose and grafted cellulose.
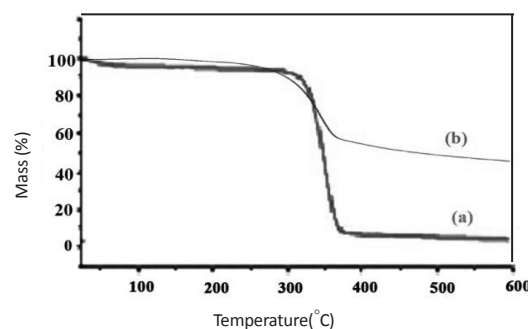

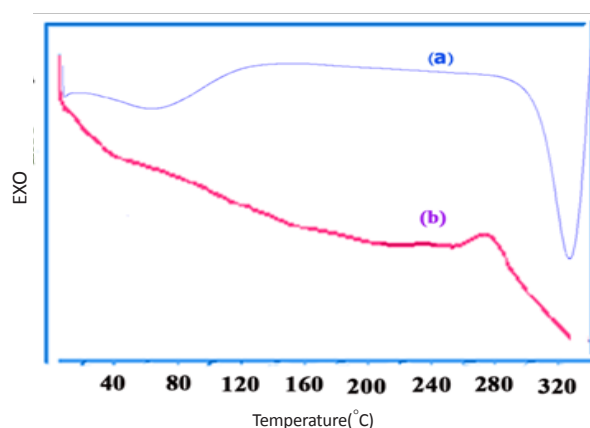**Figure 3: TGA thermograms of (a) pure cellulose and
(b) Cell-g-PS-g-PAN**

**Figure 4: DCS curves of (a) pure cellulose and
 (b) Cell-g-PS-g-PAN**

Polystyrene and polyacrylonitrile chains bonded to the backbone of cellulose lead to more flexibility in terpolymer structure and cause degradation at lower temperatures.

About 10% mass loss at $250\text{-}300°C$ in TGA and an exothermic DSC peak at around $270°C$ are observed for the grafted cellulose. In the temperature range of $300–370°C$, large mass losses are observed. The mass of cellulose has steeply decreased with temperature, while that of the grafted cellulose has been decreasing gradually, and this trend has continued to the final temperature, where the mass loss is 80% for cellulose and 33% for the grafted cellulose.

SEM Analysis

In Figure 5, the comparison of the SEM micro

graphs of unmodified cellulose [37] with that of the grafted cellulose gives a clear indication of the change in the topology of the grafted samples. Grafting of St and a monomer onto cellulose backbone opens up its matrix and shows considerable deposition of poly (AN+St) on the surface of the backbone polymers.
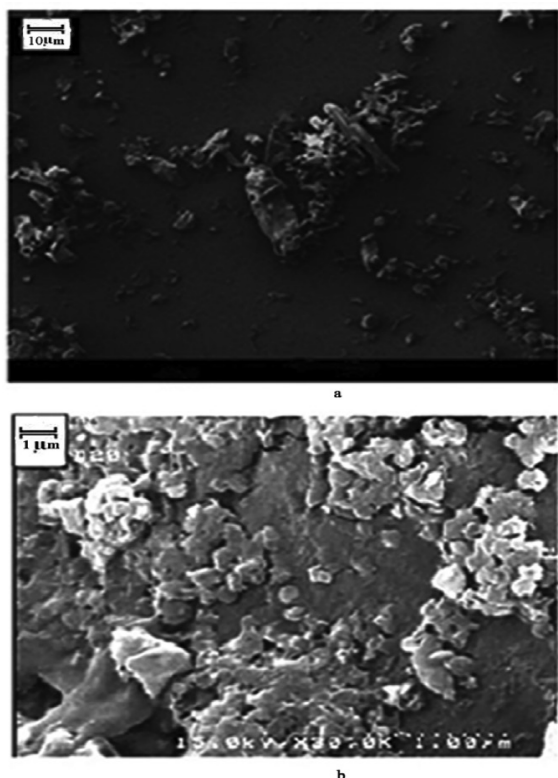

Figure 5: SEM micrographs of (a) raw cellulose and (b) Cell-g-PS-g-PAN terpolymer

Synthesis of O-MMT and Bionanocomposite

Figure 6 shows the FT-IR spectra of the unmodified MMT and O-MMT. In the spectra of both modified and unmodified clays, the intense peak at 1045 cm^{-1} and the two bands at 467 and 525 cm^{-1} have been assigned to Si-O band stretching and Si-O band bending respectively. Unreacted hexadecyl trimethyl ammonium chloride shows a characteristic peaks at 1637 which is attributed to ammonium groups. The band around 3630 cm^{-1} is due to the stretching of Si-OH groups in the clay.

The FT-IR spectrum of the modified clay exhibits an absorption band at 1473 cm^{-1} attributed to C-H bending bands of methyl groups of hexadecyl trimethyl ammonium chloride. In addition, the intercalation of modifier instead of sodium ions can be confirmed by the C-H stretching vibration at 2855 and 2925 cm^{-1}.
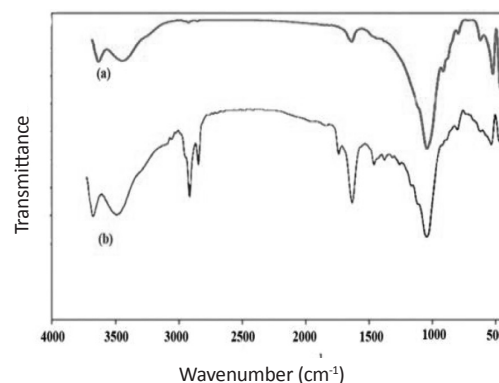

Figure 6: FT-IR spectra of (a) unmodified MMT and (b) O-MMT

Figure 7 shows the XRD patterns of the unmodified MMT, the O-MMT, and the terpolymer/clay nanocomposite. An increase in the basal spacing (d_{001}) of the O-MMT clay is observed after the insertion of the surfactant. More specifically, the pristine MMT shows a d_{001} spacing of 11.6 A˚ at 2θ = 8˚, which corresponds to an interlayer space D = 11.6–9.6 = 2 A˚; 9.6 A˚ is the thickness of the individual clay sheet. In the case of the organoclay, the basal spacing d_{001} becomes 14.2 A˚ at 2θ = 6˚, with a corresponding interlayer space of D=2.6 A˚.
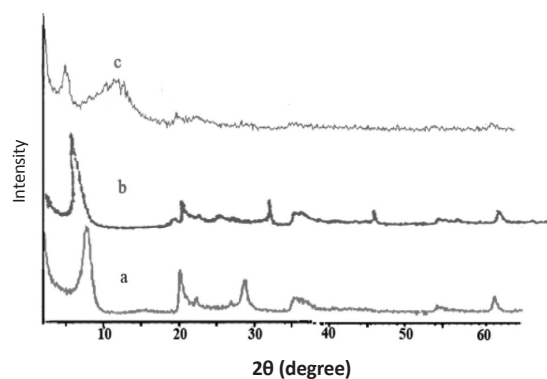

Figure 7: XRD patterns of (a) unmodified MMT, (b) O-MMT, and (c) Cell-g-PS-g-PAN /O-MMT bionanocomposites

By making a comparison between O-MMT , it is clear that the diffraction pattern of O-MMT shows the characteristic peaks at 2θ = 6°, whereas this peak has been decreased for the nanocomposite. However, the absence of XRD signals at low angles does not provide definitive proof of complete exfoliation because the silicate has been diluted by polymer. Furthermore, XRD is not quantitative in determining the amount of exfoliation versus intercalation. Figure 8 shows the SEM micrographs of terpolymer/clay nanocomposite. It is clear that silicate layers have been dispersed in polymer matrix, which might be attributed to intercalated or partially exfoliated structures. This observation is consistent with the XRD results.
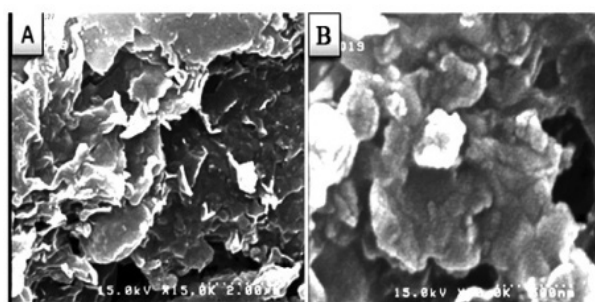

A: 2 μm
B:0.5 μm

Figure 8: SEM micrographs of Cell-g-PS-g-PAN /O-MMT bionanocomposite

The TEM images of the terpolymer/clay nanocomposite are displayed in Figure 9. The dark lines indicate the MMT layers. In Figure 9, nanosized MMT aggregates could be detected in varying degrees, which might be attributed to intercalated or partially exfoliated structures. This observation is consistent with the XRD and SEM results. If the silicates are dispersed randomly and homogeneously in the polymer matrix, the interface area is enormous and pronounced interaction can be expected.
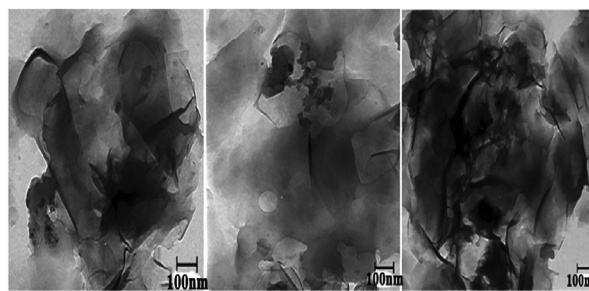

Figure 9: TEM images of the Cell-g-PS-g-PAN /O-MMT bionanocomposites

CONCLUSIONS

A novel approach to the synthesis of Cell-g-PS-g-PAN via combination of conventional and advanced methods has been demonstrated. First, styrene has been grafted onto cellulose fibers via free radical polymerization by using the suspension polymerization technique. In this process, PPS has been used as a chemical initiator, and water has been used as a medium. Then, the obtained grafted copolymer has been brominated by NBS to prepare ATRP macroinitiator. Next, this macroinitiator can polymerize AN in the presence of an ATRP catalyst system in THF solvent. Afterwards, O-MMT has been obtained after being treated with hexadecyl trimethyl ammonium chloride salt. Finally, Cell-g-PS-g-PAN/organoclay bionanocomposite has been prepared in CCl_4 by a solution intercalation method. The structure of the obtained terpolymer has been investigated by FT-IR, DSC, TGA, XRD, and SEM techniques. Moreover, the structure of the bionanocomposite has been probed by XRD, SEM, and TEM images.

ACKNOWLEDGMENTS

NOMENCLATURES

AHG : Anhydroglucose

AIBN : 2, 2'-Azobis (isobutyronitrile)

AN : Acrylonitrile

ATRP : Atom Transfer Radical Polymerization

Bpy : 2, 2'-Bipyridine

Cell : Cellulose

DSC : Differential scanning calorimetry

FTIR : Fourier-transform Infrared

G or g : Graft

MMT : Montmorillonite

NMP : Nitroxide-mediated Polymerization

O-MMT : Organo-modified Montmorillonite

PAN : Polyacrylonitrile

PS : Polystyrene

RAFT : Reversible Addition Fragmentation Process

SEM : Scanning Electron Microscopy

St : Styrene

TEM : Transmission Electron Microscopy

TGA : Thermogravimetric Analysis

Tg : Glass Transition Temperature

XRD : X-ray Diffraction

REFERENCES

1. Sinha Ray S. and Bousmina M., "Biodegradable Polymers and their Layered Silicate Nanocomposites: in Greening the 21st Century Materials World," *Progress in Material Science*, **2005**, *50*, 962–1079.
2. Armentano I., Dottori M., Fortunati E., Mattioli S. et al., "Biodegradable Polymer Matrix Nanocomposites for Tissue Engineering: a Review," *Polymer Degradation and Stability*, **2010**, *95*, 2126–2146.
3. Kotek J., Kubies D., Baldrian J., and Kovárová, J., "Biodegradable Polyester Nanocomposites: the Effect of Structure on Mechanical and Degradation Behavior," *Eur. Polym. J.*, **2011**, 47, 2197–2207.
4. Leaversuch R., "Plastics Technology [online Magazine; biomaterials and materials zone], http://www.ptonline.com/zones, Sept.3, **2002** [April 2013].
5. Fortunati E., Armentano I., Zhou Q., Iannoni A., et al., "Multifunctional Bionanocomposite Films of Poly(lactic acid), Cellulose Nanocrystals and Silver Nanoparticles," *Carbohydr. Polym.*, **2012**, 87, 1596–1605.
6. Fortunati E., Armentano I., Zhou Q., Puglia D., et al., "Microstructure and Nonisothermal Cold Crystallization of PLA Composites Based on Silver Nanoparticles and Nanocrystalline Cellulose," *Polym. Degrad. Stabil.*, **2012**, *97*, 2027–2036.
7. Darder M., Aranda P., and Ruiz-Hitzky E., "Bionanocomposites: a New Concept of Ecological, Bioinspired, and Functional Hybrid Materials," *Adv. Mater.*, **2007**, *19*, 1309–1319.
8. Raka L., Bogoeva-Gaceva G., Lu K., and Loos J., "Characterization of Latex-based Isotactic Polypropylene/Clay Nanocomposites," *Polymer*, **2009**, *50*, 3739–3746.
9. Jaymand, M., "Surface Modification of Montmorillonite with Novel Modifier and Preparation of Polystyrene/ Montmorillonite Nanocomposite by In Situ Radical Polymerization," *J. Polym. Res.*, **2011**, *18*, 957–963.
10. Klemm D., Heublein B., Fink H-P., and Bohn A., "Cellulose: Fascinating Biopolymer and Sustainable Raw Material," *Angew Chem. Int. Ed.*, **2005**, *44*, 3358-3393.
11. Simkovic I., "What Could Be Greener than Composites Made from Polysaccharides," *Carbohydr. Polym.*, **2008**, *74*, 759-762.
12. Bredereck K. and Hermanutz F., "Man- Made Cellulosics," *Rev. Prog. Color. Relat. Top.*, **2005**, *35*, 59-75.
13. Klemm D., Philipp B., Heinze T., Heinze U., et al., "Comprehensive Cellulose Chemistry," Wiley-VCH, Germany, **1998**.
14. Hebeish A. and Guthrie J. T., "The Chemistry and Technology of Cellulosic Copolymers," Springer-Verlag, Berlin, **1981**.
15. Khan F., "Photoinduced Graft-copolymer Synthesis and Characterization of Methacrylic Acid onto Natural Biodegradable Lignocellulose Fiber,"

Biomacromolecules, **2004**, *5*, 1078–1088

16. Roy D., Semsarilar M., Guthrie J. T., and Perrier S., "Cellulose Modification by Polymer Grafting: a Review," *Chem. Soc. Rev.*, **2009**, *38*, 2046–2064.

17. Xia J., and Matyjaszewski K., "Controlled /"Living" Radical Polymerization Atom Transfer Radical Polymerization Using Multidentate Amine Ligands," *Macromolecules*, **1997**, *30*, 7697-7700.

18. Koenig, H. S. and Roberts C. W., "Vinylbenzyl Ethers of Cellulose. Preparation and Polymerization," *J. Appl. Polym. Sci.*, **1974**, *18*, 651–666.

19. Abbasian M. and Esmaeily Shoja Bonab S., "Nitroxide Mediated and Atom Transfer Radical Graft Polymerization of Atactic Polymers onto Syndiotactic Polystyrene," *Braz. J. Chem. Eng.*, **2012**, *29*, 285-294.

20. Abbasian M., Esmaeily Shoja S., and Shahparian M., "Chemical Modification of Polypropylene by Nitroxide Mediated Living Radical Graft Polymerization of Styrene," *Iran. Polym. J.*, **2013**, *22*, 209-218.

21. Abbasian M. and Mahi R., "In Situ Synthesis of Polymer-silica Nanocomposites by Living Radical Polymerization Using TEMPO Initiator," *J. Exp. Nanosci.*, **2014**, *9*, 785-798.

22. Barner L., "Surface Grafting via the Reversible Addition Fragmentation Chain Transfer (RAFT) Process: from Polypropylene Beads to Core-shell Microspheres," *Aust. J. Chem.*, **2003**, *56*, 1091.

23. Perrier S., Takolpuckdee P., Westwood J., and Lewis D. M., "Versatile Chain Transfer Agents for Reversible Addition Fragmentation Chain Transfer (RAFT) Polymerization to Synthesize Functional Polymeric Architectures," *Macromolecules*, **2004**, *37*, 2709–2717.

24. Takolpuckdee P., "Chain Transfer Agents for RAFT Polymerization: Molecules to Design Functionalized Polymers," *Aust. J. Chem.*, **2005**, *58*, 66–66.

25. Abbasian M., Esmaeily Shoja S., and Shahparian M., "Synthesis of PMMA-graft-MAH-graftPP/organoclay Nanocomposites via Metal Catalyzed Radical Polymerization and Solvent Blending Methods," *Polym. Plast. Technol. Eng.*, **2012**, *51*, 1589-159

26. Abbasian M., Fathi A., Entezami A. A., and Jaymand M., "Preparation and Characterization of Hyperbranched Polystyrene Nanocomposite Synthesized by Living Radical Polymerization and Solution Intercalation Method," *Iran. J. Polym. Sci. Technol.*, **2012**, *24*, 433- 443.

27. Abbasian M. and Khakpour Ali N, "Synthesis of Poly (methyl methacrylate)/Zinc Oxide Nanocomposite with Core-shell Morphology by Atom Transfer Radical Polymerization," *J. Macromol. Sci, Pure. Appl. Chem.*, **2013**, *50*, 966-975.

28. Summerlin B. S, Tsarevsky N. V., Louche G., Matyjaszewski K., et al., "Highly Efficient "Click" Functionalization of Poly (3-Azidopropylmethacrylate) Prepared by ATRP," *Macromolecules*, **2005**, *38*, 7540-7545.

29. Sinha Ray S. and Okamoto M., "Polymer/ Layered Silicate Nanocomposites: a Review from Preparation to Processing," *Prog. Polym. Sci.*, **2003**, *28*, 1539–1641.

30. Jiang G., Huang H. X., and Chen Z. K., "Microstructure and Thermal Behavior of Polylactide / Clay Nanocomposites Melt Compounded under Supercritical CO_2," *Adv. Polym. Tech.*, **2011**, *30*, 174-182.

31. Urbanczyk L., Ngoundjo F., Alexandre M., Jerome C., et al., "Synthesis of Polylactide/ Clay Nanocomposites by In Situ Intercalative Polymerization in Supercritical Carbon Dioxide," *Eur. Polym. J.*, **2009**, *45*, 643–648.

32. Moad G. and Solomon D. H., "The Chemistry of Radical Polymerization," Elsevier Ltd, Oxford, **2006**.

33. Ibrahim M. D., Mondal H., Uraki Y., Ubukata M. et al., "Graft Polymerization of Vinyl Monomers onto Cotton Fibers Pretreated with Amines," *Cellulose*, **2008**, *15*, 581–592.

34. Lin C. X., Zhan H. U., Liu M. H., Fu S. U., et al., "Rapid Homogeneous Preparation of Cellulose Graft Copolymer in BMIMCL under Microwave Irradiation," *J. Appl. Polym. Sci.*, **2010**, *118*, 399-404.

35. Toledano-Thompson T., Loria- Bastarrachea M. I., and Aguilar-Vega M. J., "Characterization of Henequen

Cellulose Microfibers Treated with an Epoxide and Grafted with Poly(acrylic acid)," *Carbohyd. Polym.*, **2005**, *62*, 67–73.

36. Ghosh P. and Das D., "Modification of Cotton by Acrylic Acid (AA) in the Presence of NaH_2PO_4 and $K_2S_2O_8$ as Catalysts under Thermal Treatment," *Eur. Polym. J.*, **2000**, *36*, 2505-2511.

37. De Oliveira R. L., Da Silva Barud H., D Assuncao R. M. N., Da Silva Meireles C. et al., "Synthesis and Characterization of Microcrystalline Cellulose Produced from Bacterial Cellulose," *J. Therm. Anal. Calorim.*, **2011**, *106*, 703–709.

38. El-Khouly A.S., Takahashi Y., Takada A., Safaan A. A. et al., "Characterization and Thermal Stability of Cellulose-graft- Polyacrylonitrile Prepared by Using $KMnO_4$/Citric Acid Redox System," *J. Appl. Polym. Sci.*, **2010**, *116*, 1788-1795.